Inorganic Chemistry
Article

Inorg. Chem. **2009**, *48*, 11277–11282 **11277**
DOI: 10.1021/ic901770e

Noncentrosymmetry in New Templated Gallium Fluorophosphates

Sarah J. Choyke,[†] Samuel M. Blau,[†] Abigail A. Larner,[†] Amy Narducci Sarjeant,[‡] Jeongho Yeon,[§] P. Shiv Halasyamani,[§] and Alexander J. Norquist*[,†]

[†]*Department of Chemistry, Haverford College, Haverford, Pennsylvania 19041,* [‡]*Department of Chemistry, Northwestern University, Evanston, Illinois 60208, and* [§]*Department of Chemistry, University of Houston, Houston, Texas 77204*

Received September 4, 2009

Two new noncentrosymmetric polar gallium fluorophosphates have been synthesized under mild hydrothermal conditions through the use of enantiomorphically pure sources of either R-2-methylpiperazine or S-2-methylpiperazine. A centrosymmetric analogue was also prepared using a racemic source of the amine. Novel $[Ga_3F(PO_4)_4]_n^{4n-}$ layers, constructed from $[Ga_3O_3F(PO_4)_4]$ building units, are observed in all three compounds. The use of racemic 2-methylpiperazine results in crystallographic disorder of the amines and creation of inversion centers, while using a single enantiomer destroys the inversion symmetry and orders the amines. Second harmonic generation measurements were performed on $[(R)\text{-}C_5H_{14}N_2]_2[Ga_3F(PO_4)_4]\cdot 5.5H_2O$ and $[(S)\text{-}C_5H_{14}N_2]_2[Ga_3F(PO_4)_4]\cdot 4.75H_2O$, both of which display type 1 phase-matching capabilities and exhibit activities of $\sim 50 \times \alpha\text{-}SiO_2$. The structures of these compounds were determined using single crystal X-ray diffraction, infrared spectroscopy, and thermal analyses. $[C_5H_{14}N_2]_2[Ga_3F(PO_4)_4]\cdot 5.25H_2O$, a = 13.0863(5) Å, c = 9.9023(4) Å, trigonal, $P\bar{3}$ (No. 147), Z = 2; $[(R)\text{-}C_5H_{14}N_2]_2[Ga_3F(PO_4)_4]\cdot 5.5H_2O$, a = 13.0887(2) Å, c = 29.9439(4) Å, trigonal, $P3_1$ (No. 144), Z = 6; $[(S)\text{-}C_5H_{14}N_2]_2[Ga_3F(PO_4)_4]\cdot 4.75H_2O$, a = 13.0871(2) Å, c = 29.8350(6) Å, trigonal, $P3_2$ (No. 145), Z = 6.

Introduction

Materials that possess crystallographic noncentrosymmetry (NCS) are of great interest to researchers because they can exhibit several desirable physical properties,[1] including nonlinear optical activity such as second harmonic generation (SHG) or frequency doubling and piezoelectricity. Despite the crystallographic requirements for the possibility of these properties, the performances of specific compounds are determined by structure and composition.

The ability to form NCS structures from chiral components was first observed qualitatively by Pasteur.[2,3] The orientation of the hemihedral facets in crystals of sodium ammonium tartrate reflected the chirality of the tartrate anions as well as noncentrosymmetry and enantiomorphism of the three-dimensional structure (space group $P2_12_12$).[4,5] However, the extension of this technique to systems containing metal oxide components is both more desirable and more difficult.

Noncentrosymmetric compounds containing metal oxide bonds are of specific interest because of their high polarizabilities, the suspected source of the unusually high SHG responses in materials such as $KTiOPO_4$ (KTP)[6,7] and $LiNbO_3$.[8] Such materials have been synthesized using chiral components, either through direct incorporation of chiral coordination complexes,[9] amino acids,[10] and organic amines[11−15] or through induction using chiral ionic liquids.[16] Other strategies for the formation of novel NCS compounds include the use of second-order Jahn−Teller cations,[6−8] main group cations with stereochemically active lone pairs,[17−19] and inherently acentric metal oxide

*Author to whom correspondence should be addressed.

(1) Halasyamani, P. S.; Poeppelmeier, K. R. *Chem. Mater.* **1998**, *10*, 2753–2769.
(2) Pasteur, L. *Ann. Chim. Phys.* **1848**, *24*, 442–459.
(3) Pasteur, L. *Ann. Chim. Phys.* **1850**, *28*, 56–99.
(4) Beevers, C. A.; Hughes, W. *Proc. Royal Soc. London, Series A* **1941**, *177*, 251–259.
(5) Kuroda, R.; Mason, S. F. *J. Chem. Soc., Dalton Trans.* **1981**, 1268–1273.
(6) Jeggo, C. R.; Boyd, G. D. *J. Appl. Phys.* **1970**, *41*, 2741–2743.
(7) Levine, B. F. *Phys. Rev. B* **1973**, *7*, 2600–2626.
(8) Chen, C. T.; Liu, G. Z. *Annu. Rev. Mater. Sci.* **1986**, *16*, 203–243.
(9) Kepert, C. J.; Prior, T. J.; Rosseinsky, M. J. *J. Am. Chem. Soc.* **2000**, *122*, 5158–5168.
(10) Inoue, M.; Yamase, T. *Bull. Chem. Soc. Jpn.* **1995**, *68*, 3055–3063.
(11) Nenoff, T. M.; Thoma, S. G.; Provencio, P.; Maxwell, R. S. *Chem. Mater.* **1998**, *10*, 3077–3080.
(12) Lin, H.-M.; Lii, K.-H. *Inorg. Chem.* **1998**, *37*, 4220–4222.
(13) Gutnick, J. R.; Muller, E. A.; Sarjeant, A. N.; Norquist, A. J. *Inorg. Chem.* **2004**, *43*, 6528–6530.
(14) Muller, E. A.; Cannon, R. J.; Sarjeant, A. N.; Ok, K. M.; Halasyamani, P. S.; Norquist, A. J. *Cryst. Growth Des.* **2005**, *5*, 1913–1917.
(15) Veltman, T. R.; Stover, A. K.; Sarjeant, A. N.; Ok, K. M.; Halasyamani, P. S.; Norquist, A. J. *Inorg. Chem.* **2006**, *45*, 5529–5537.
(16) Lin, Z.; Slawin, A. M. Z.; Morris, R. E. *J. Am. Chem. Soc.* **2007**, *129*, 4880–4881.
(17) Harrison, W. T. A.; Dussack, L. L.; Jacobson, A. J. *J. Solid State Chem.* **1996**, *125*, 234–242.
(18) Ok, K. M.; Halasyamani, P. S. *Chem. Mater.* **2002**, *14*, 2360–2364.
(19) Sykora, R. E.; Ok, K. M.; Halasyamani, P. S.; Wells, D. M.; Albrecht-Schmitt, T. E. *Chem. Mater.* **2002**, *14*, 2741–2749.

Published on Web 10/28/2009

fluoride anions.[20,21] In addition, several metal organic frameworks containing acentric linkers,[22,23] compounds composed of mixed ionic and covalent sublattices synthesized using salt-inclusion reactions,[24,25] and structurally related tungsten bronzes,[26] borates,[27−29] and KTP-type gallium fluorophosphates[30,31] are noncentrosymmetric.

A host of organically templated gallium phosphates and fluorophosphates have been reported in the past 15 years.[32−39] This mature system contains an exceptionally diverse range of inorganic architectures and has yielded valuable information about formation mechanisms in such compounds.[34,40,41] We report the use of chiral organic amines to direct crystallographic noncentrosymmetry in a series of novel gallium phosphates. The synthesis, structure, and characterization of three new organically templated gallium fluorophosphates are reported. A previously unreported $[Ga_3F(PO_4)_4]_n^{4n-}$ layer topology is observed in each compound. $[C_5H_{14}N_2]_2[Ga_3F(PO_4)_4]\cdot 5.25H_2O$ (**1**) was synthesized using racemic 2-methylpiperazine and is centrosymmetric, while the noncentrosymmetric compounds $[(R)\text{-}C_5H_{14}N_2]_2[Ga_3F(PO_4)_4]\cdot 5.5H_2O$ (**2**) and $[(S)\text{-}C_5H_{14}N_2]_2[Ga_3F(PO_4)_4]\cdot 4.75H_2O$ (**3**) were synthesized using enantiomerically pure sources of (R)-2-methylpiperazine and (S)-2-methylpiperazine, respectively. Compounds **2** and **3** are both active for second harmonic generation and display type 1 phase-matching capabilities, and efficiencies of approximately 50 × α-SiO_2.

Experimental Section

Materials. $Ga(NO_3)_3\cdot H_2O$ (99.9%), H_3PO_4 (85%), 2-methylpiperazine (95%, 2-mpip), (R)-(-)-2-methylpiperazine (97%, R-2-mpip), (S)-(+)-2-methylpiperazine (99%, S-2-mpip), and HF_{aq} (48%) were purchased from Aldrich and used as received. Deionized water was used in these syntheses.

Synthesis. All reactions were conducted in 23 mL poly(fluoroethylene-propylene) lined pressure vessels. Reactions were heated to 150 °C over 30 min and allowed to soak for 4 days. The reactions were then cooled to room temperature at a rate of 6 °C h^{-1} to promote the growth of large single crystals. Autoclaves were opened in air, and products were recovered through filtration. Reaction yields ranged between 55−60% based on Ga. No additional reaction products other than those described below, crystalline or amorphous, were observed.

$[C_5H_{14}N_2]_2[Ga_3F(PO_4)_4]\cdot 5.25H_2O$ (1). Compound **1** was synthesized through the reaction of 0.0740 g (2.70×10^{-4} mol) of $Ga(NO_3)_3\cdot H_2O$, 0.2552 g (2.90×10^{-3} mol) of 2-mpip, 0.3085 g (3.18×10^{-3} mol) of H_3PO_4, 2 drops (~0.2 g, 1.0×10^{-3} mol) of HF_{aq}, and 3.0087 g (1.67×10^{-1} mol) of deionized water. Colorless blocks. Elemental microanalysis for **1** obsd (calc): C 13.66(13.24); H 4.16(4.25); N 6.20(6.18). IR data: N − H 1465, 1499, 1629 cm^{-1}, C − H 3020 cm^{-1}, P − O 1022, 1102 cm^{-1}.

$[(R)\text{-}C_5H_{14}N_2]_2[Ga_3F(PO_4)_4]\cdot 5.5H_2O$ (2). Compound **2** was synthesized through the reaction of 0.0758 g (2.77×10^{-4} mol) of $Ga(NO_3)_3\cdot H_2O$, 0.2565 g (2.91×10^{-3} mol) of R-2-mpip, 0.3057 g (3.12×10^{-3} mol) of H_3PO_4, 2 drops (~0.2 g, 1.0×10^{-3} mol) of HF_{aq}, and 3.0057 g (1.67×10^{-1} mol) of deionized water. Colorless blocks. Elemental microanalysis for **2** obsd (calc): C 13.52(13.17); H 4.19(4.28); N 6.14(6.15). IR data: N − H 1466, 1499, 1628 cm^{-1}, C − H 3019 cm^{-1}, P − O 1020, 1096 cm^{-1}.

$[(S)\text{-}C_5H_{14}N_2]_2[Ga_3F(PO_4)_4]\cdot 4.75H_2O$ (3). Compound **3** was synthesized through the reaction of 0.0746 g (2.73×10^{-4} mol) of $Ga(NO_3)_3\cdot H_2O$, 0.2575 g (2.93×10^{-3} mol) of S-2-mpip, 0.3029 g (3.09×10^{-3} mol) of H_3PO_4, 2 drops (~0.2 g, 1.0×10^{-3} mol) of HF_{aq}, and 3.0029 g (1.67×10^{-1} mol) of deionized water. Colorless blocks. Elemental microanalysis for **3** obsd (calc): C 13.40(13.37); H 4.15(4.18); N 6.10(6.24). IR data: N − H 1458, 1496 cm^{-1}, C − H 3019 cm^{-1}, P − O 1022, 1100 cm^{-1}.

Single Crystal X-ray Diffraction. Data were collected using an Oxford Diffraction Xcalibur3 CCD diffractometer with an Enhance Mo Kα radiation source (λ = 0.71073 Å). A single crystal was mounted on a glass fiber using N-paratone oil and cooled in situ to 110(2) K for data collection. Frames were collected, indexed, and processed, and the files were scaled using CrysAlis RED.[42] The heavy atom positions were determined using SIR92.[43] All other non-hydrogen sites were located from Fourier difference maps. All non-hydrogen sites were refined using anisotropic thermal parameters using the full matrix least-squares procedures on F_o^2 with $I > 3\sigma(I)$. Hydrogen atoms were placed in geometrically idealized positions. All calculations were performed using Crystals.[44] Relevant crystallographic data are listed in Table 1.

Powder X-ray Diffraction. Powder diffraction patterns were recorded on a GBC-Difftech MMA powder diffractometer. Samples were mounted on aluminum plates. Calculated powder patterns were generated from single crystal data using ATOMS v. 6.0.[45]

Infrared Spectroscopy. Infrared measurements were obtained using a PerkinElmer FT-IR Spectrum 1000 spectrophotometer. Samples were diluted with spectroscopic grade KBr and pressed into a pellet. Scans were run over the range of 400−4000 cm^{-1}.

Thermogravimetric Analysis. Thermogravimetric analyses (TGA) were conducted using a TGA 2050 thermogravimetric analyzer from TA Instruments. Samples were contained within a platinum crucible and heated in nitrogen at 10 °C min^{-1} to 800 °C. TGA traces are available in the Supporting Information.

(20) Maggard, P. A.; Stern, C. L.; Poeppelmeier, K. R. *J. Am. Chem. Soc.* **2001**, *123*, 7742–7743.
(21) Marvel, M. R.; Lesage, J.; Baek, J.; Halasyamani, P. S.; Stern, C. L.; Poeppelmeier, K. R. *J. Am. Chem. Soc.* **2007**, *129*, 13963–13969.
(22) Evans, O. R.; Lin, W. *Acc. Chem. Res.* **2002**, *35*, 511–522.
(23) Moulton, B.; Zaworotko, M. J. *Chem. Rev.* **2001**, *101*, 1629–1658.
(24) Hwu, S.-J.; Ulutagay-Kartin, M.; Clayhold, J. A.; Mackay, R.; Wardojo, T. A.; O'Connor, C. J.; Krawiec, M. *J. Am. Chem. Soc.* **2002**, *124*, 12404–12405.
(25) Huang, Q.; Hwu, S.-J. *Inorg. Chem.* **2003**, *42*, 655–657.
(26) Chi, E. O.; Gandini, A.; Ok, K. M.; Zhang, L.; Halasyamani, P. S. *Chem. Mater.* **2004**, *16*, 3616–3622.
(27) Knyrim, J. S.; Becker, P.; Johrendt, D.; Huppertz, H. *Angew. Chem., Int. Ed.* **2006**, *45*, 8239–8241.
(28) Pan, S.; Wu, Y.; Fu, P.; Zhang, G.; Li, Z.; Du, C.; Chen, C. *Chem. Mater.* **2003**, *15*, 2218–2221.
(29) Chen, C.; Wang, Y.; Wu, B.; Wu, K.; Zeng, W.; Yu, L. *Nature* **1995**, *374*, 290.
(30) Harrison, W. T. A.; Phillips, M. L. F.; Stucky, G. D. *Chem. Mater.* **1995**, *7*, 1849–1856.
(31) Loiseau, T.; Paulet, C.; Simon, N.; Munch, V.; Taulelle, F.; Ferey, G. *Chem. Mater.* **2000**, *12*, 1393–1399.
(32) Bonhomme, F.; Thoma, S. G.; Nenoff, T. M. *J. Mater. Chem.* **2001**, *11*, 2559–2563.
(33) Bonhomme, F.; Thoma, S. G.; Rodriguez, M. A.; Nenoff, T. M. *Chem. Mater.* **2001**, *13*, 2112–2117.
(34) Ferey, G. *J. Fluorine Chem.* **1995**, *72*, 187–193.
(35) Ferey, G. *C. R. Acad. Sci., Ser. IIc: Chim.* **1998**, *1*, 1–13.
(36) Loiseau, T.; Ferey, G. *J. Fluorine Chem.* **2007**, *128*, 413–422.
(37) Sassoye, C.; Loiseau, T.; Ferey, G.; Taulelle, F. *Chem. Commun.* **2000**, 943–944.
(38) Wragg, D. S.; Morris, R. E. *J. Phys. Chem. Solids* **2001**, *62*, 1493–1497.
(39) Weigel, S. J.; Weston, S. C.; Cheetham, A. K.; Stucky, G. D. *Chem. Mater.* **1997**, *9*, 1293–1295.
(40) Ferey, G. *Chem. Mater.* **2001**, *13*, 3084–3098.
(41) Rao, C. N. R.; Natarajan, S.; Choudhury, A.; Neeraj, S.; Ayi, A. A. *Acc. Chem. Res.* **2001**, *34*, 80–87.
(42) *CrysAlis CCD and CrysAlis RED*, version 1.171; Oxford Diffraction, Ltd.: Abdingdon, UK, 2002
(43) Altomare, A.; Cascarano, G.; Giacovazzo, C.; Guagliardi, A. *J. Appl. Crystallogr.* **1993**, *26*, 343–350.
(44) Betteridge, P. W.; Carruthers, J. R.; Cooper, R. I.; Prout, K.; Watkin, D. J. *J. Appl. Crystallogr.* **2003**, *36*, 1487.
(45) Dowty, E. *ATOMS*, version 6.0; Shape Software , Kinsgsport, TN, 2002

Table 1. Crystallographic Data for Compounds **1**−**3**

compound	$[C_5H_{14}N_2]_2[Ga_3F(PO_4)_4]\cdot 5.25H_2O$ (**1**)	$[(R)\text{-}C_5H_{14}N_2]_2[Ga_3F(PO_4)_4]\cdot 5.5H_2O$ (**2**)	$[(S)\text{-}C_5H_{14}N_2]_2[Ga_3F(PO_4)_4]\cdot 4.75H_2O$ (**3**)
formula	$C_{10}H_{38.5}FGa_3N_4O_{21.25}P_4$	$C_{10}H_{39}FGa_3N_4O_{21.5}P_4$	$C_{10}H_{37.5}FGa_3N_4O_{20.75}P_4$
fw	906.56	911.06	897.56
space group	*P*-3 (No. 147)	$P3_1$ (No. 144)	$P3_2$ (No. 145)
a (Å)	13.0863(5)	13.0887(2)	13.0871(2)
b (Å)	13.0863(5)	13.0887(2)	13.0871(2)
c (Å)	9.9023(4)	29.8439(4)	29.8350(6)
α (deg)	90	90	90
β (deg)	90	90	90
γ (deg)	120	120	120
V (Å^3)	1468.59(10)	4427.71(11)	4425.31(13)
Z	2	6	6
ρ_{calc} (g cm^{-3})	2.006	2.026	2.000
λ (Å)	0.71073	0.71073	0.71073
T (K)	110(2)	110(2)	110(2)
μ (mm^{-1})	3.048	3.036	3.034
Flack parameter	−	0.019(14)	0.063(16)
R_1[a]	0.0373	0.0411	0.0421
wR_2[b]	0.0742	0.1370	0.1005

[a] $R_1 = \sum||F_o| - |F_c||/\sum|F_o|$. [b] $wR_2 = [\sum w(F_o^2 - F_c^2)^2/[\sum w(F_o^2)^2]^{1/2}$.

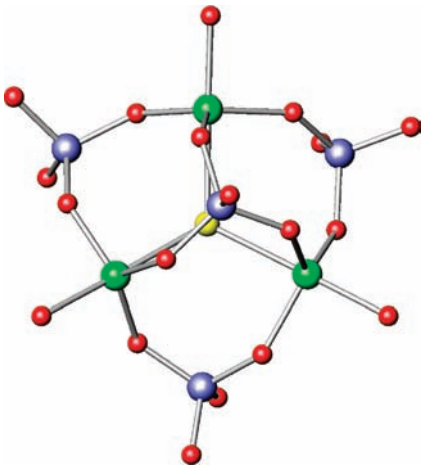

Figure 1. $[Ga_3O_3F(PO_4)_4]$ secondary building units in compounds **1**−**3**. Green, blue, yellow, and red spheres represent gallium, phosphorus, fluorine, and oxygen atoms, respectively.

Nonlinear Optical Measurements. Powder SHG measurements were conducted using a modified Kurtz-NLO system with a 1064 nm light source.[46,47] Polycrystalline $[(R)\text{-}C_5H_{14}N_2]_2[Ga_3F(PO_4)_4]\cdot 5.5H_2O$ and $[(S)\text{-}C_5H_{14}N_2]_2[Ga_3F(PO_4)_4]\cdot 4.75H_2O$ were ground and sieved into distinct particle size ranges: < 20, 20−45, 45−63, 63−75, 75−90, and 90−120 *μ*m. Crystalline α-quartz was ground and sieved into identical particle size ranges in order to compare the SHG properties of $[(R)\text{-}C_5H_{14}N_2]_2[Ga_3F(PO_4)_4]\cdot 5.5H_2O$ (**2**) and $[(S)\text{-}C_5H_{14}N_2]_2[Ga_3F(PO_4)_4]\cdot 4.75H_2O$ (**3**) to known materials. All powders were placed in separate capillary tubes, and no index-matching fluid was used in any experiment. The SHG, i.e., 532 nm light, was collected in reflection and detected using a photomultiplier tube. A 532 nm narrow-bandpass interference filter was attached to the tube in order to only detect SHG light.

Results

$[C_5H_{14}N_2]_2[Ga_3F(PO_4)_4]\cdot 5.25H_2O$ (**1**), $[(R)\text{-}C_5H_{14}N_2]_2[Ga_3F(PO_4)_4]\cdot 5.5H_2O$ (**2**), and $[(S)\text{-}C_5H_{14}N_2]_2[Ga_3F(PO_4)_4]\cdot 4.75H_2O$ (**3**) all contain $[Ga_3O_3F(PO_4)_4]$ secondary building units[34,40] through which crystallization is thought to occur via a charge density matching process[48,49] (Figure 1). The Ga−F bond lengths range between 2.116(4) and 2.400(5) Å. Ga−O bonds that are *trans* to fluoride positions exhibit longer lengths [1.859(6)−1.892(6) Å] and other Ga−O bonds [1.807(6)−1.851(6) Å]. Condensation of the $[Ga_3O_3F(PO_4)_4]$ units results in the formation of $[Ga_3F(PO_4)_4]_n^{4n-}$ layers, which are previously unreported (Figure 2). While the $[Ga_3O_3F(PO_4)_4]$ monomer units in compounds **1**−**3** have been observed previously in Mu-34,[50] the layers in Mu-34 contain $[Ga_3O_3F(PO_4)_4]$ and $[Ga_3O_3(PO_4)_4]$ motifs and exhibit a distinctly different layer topology with respect to compounds **1**−**3**. Bond valence sums[51,52] were calculated for compounds **1**−**3**. The values on the Ga^{3+} and P^{5+} centers range between 3.10 and 3.19, and 4.73 and 4.92, respectively, in good agreement with the assigned oxidation states.

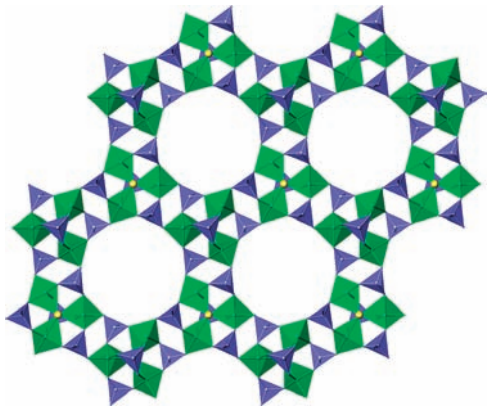

Figure 2. Polyhedral representation of the $[Ga_3F(PO_4)_4]_n^{4n-}$ layers present in **1**−**3**. Green trigonal bipyramids and blue tetrahedra represent $[GaO_4F]$ and $[PO_4]$, respectively.

(46) Kurtz, S. K.; Perry, T. T. *J. Appl. Phys.* **1968**, *39*, 3798–3813.
(47) Porter, Y.; Ok, K. M.; Bhuvanesh, N. S. P.; Halasyamani, P. S. *Chem. Mater.* **2001**, *13*, 1910–1915.
(48) Maggard, P. A.; Boyle, P. D. *Inorg. Chem.* **2003**, *42*, 4250–4252.
(49) Casalongue, H. S.; Choyke, S. J.; Sarjeant, A. N.; Schrier, J.; Norquist, A. J. *J. Solid State Chem.* **2009**, *182*, 1297–1303.
(50) Lakiss, L.; Simon-Masseron, A.; Porcher, F.; Patarin, J. *Eur. J. Inorg. Chem.* **2006**, 237–243.
(51) Brown, I. D.; Altermatt, D. *Acta Crystallogr., Sect. B* **1985**, *41*, 244–247.
(52) Brese, N. E.; O'Keeffe, M. *Acta Crystallogr., Sect. B* **1991**, *47*, 192–197.

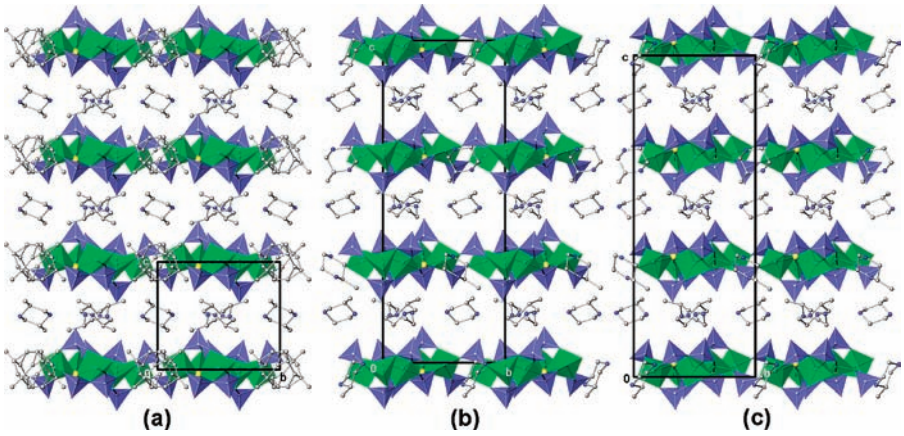

Figure 3. Three-dimensional packing of **1**−**3**. White and blue spheres represent carbon and nitrogen, respectively. Occluded water molecules and hydrogen atoms have been removed for clarity. Unit cells are shown.

Full tables of bond valence sums are available in the Supporting Information.

Compounds **1**−**3** all contain a significant number of highly disordered occluded water molecules that occupy channels in the structures. Packing figures showing these disordered water molecules are available in the Supporting Information. The number of occluded water molecules was determined for each compound using elemental analyses, thermogravimetric analyses, and diffraction studies. Each compound exhibits a characteristic mass loss between approximately 40 and 180 °C, corresponding to the loss of disordered intrachannel water molecules. Good agreement was observed between the calculated number of solvent waters using elemental analysis and TGA data. These water levels were incorporated into the final structural model on the basis of single crystal X-ray diffraction data, resulting in converged refinements for each structure.

The structures of compounds **1**−**3** are closely related. Each contains the same $[Ga_3F(PO_4)_4]_n^{4n-}$ layers, similar layer stacking, and channels occupied by disordered water molecules and $[2\text{-mpipH}_2]^{2+}$ cations. However, their symmetries differ greatly. Compound **1**, which was synthesized using racemic 2-mpip, crystallizes in the centrosymmetric space group *P*-3 (No. 144). In contrast, compounds **2** and **3** each crystallize in the noncentrosymmetric polar space groups $P3_1$ (No. 144) and $P3_2$ (No. 145), respectively. In addition, the unit cells for compounds **2** and **3** can be considered supercells of compound **1**, in which the length of the *c*-axis is tripled (Figure 3). The primary differences between compounds **2** and **3** are the presence of only R-2-mpip in **2** and only S-2-mpip in **3** and the direction of the screw axis. In both compounds, ordered $[2\text{-mpipH}_2]^{2+}$ cations and $[Ga_3O_3F(PO_4)_4]$ monomers stack along either 3_1 or 3_2 screw axes (Figure 4).

The reduction in symmetry of compounds **2** and **3** with respect to compound **1** is also reflected in the internal structure of the $[Ga_3F(PO_4)_4]_n^{4n-}$ layers. Inspection of the Ga−F bonds in these compounds is particularly revealing. A single unique Ga−F bond length of 2.2788(9) Å is observed in **1**. In contrast, six distinct Ga−F bonds are present in **2** and **3**. In **2**, the Ga−F bonds range between 2.224(4) and 2.308(4) Å for F1 and between 2.116(4) and 2.395(4) Å for F2. Similarly, the Ga−F bonds in **3** range between 2.119(5) and 2.400(5) Å for F1 and between 2.215(4) and 2.300(5) Å for F2. The marked asymmetry in the fluoride coordination geometries in **2** and **3** is a direct result of the inclusion of enantiomorphically pure amines and reflects a true reduction in symmetry of the layers.

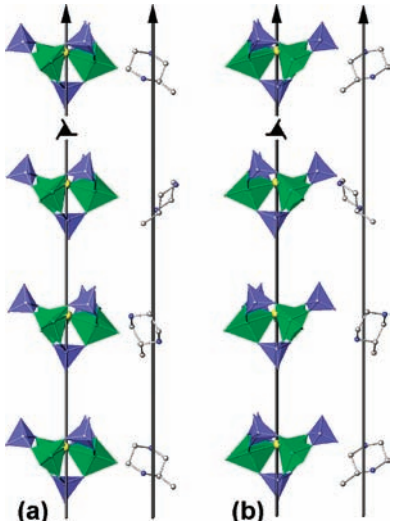

Figure 4. 3_1 and 3_2 screw axis positions in (a) **2** and (b) **3**.

The SHG intensities versus particle size for **2** and **3** are shown in Figure 5. Compounds **2** and **3** exhibit SHG intensities that are ∼50 × α−SiO_2 (the reference used in this study), and both compounds display type 1 phase-matching capabilities.

Discussion

Initial studies were conducted using a racemic source of the chiral amine 2-mpip, from which compound **1** was formed. Subsequent reactions were focused on the studying the effects of using enantiomorphically pure sources of either R-2-mpip or S-2-mpip. As noted above, the use of chiral organic amines to favor the formation of new noncentrosymmetric materials is known.[11−15,53] However, the progression from syntheses using racemic to enantiomorphically pure chiral amines is complex. The role of crystallographic order and disorder must be addressed.

The compound 2-mpip was selected for use in this study because this rigid diamine is not likely to exhibit orientational

(53) Hubbard, D. J.; Johnston, A. R.; Sanchez Casalongue, H.; Sarjeant, A. N.; Norquist, A. J. *Inorg. Chem.* **2008**, *47*, 8518–8525.

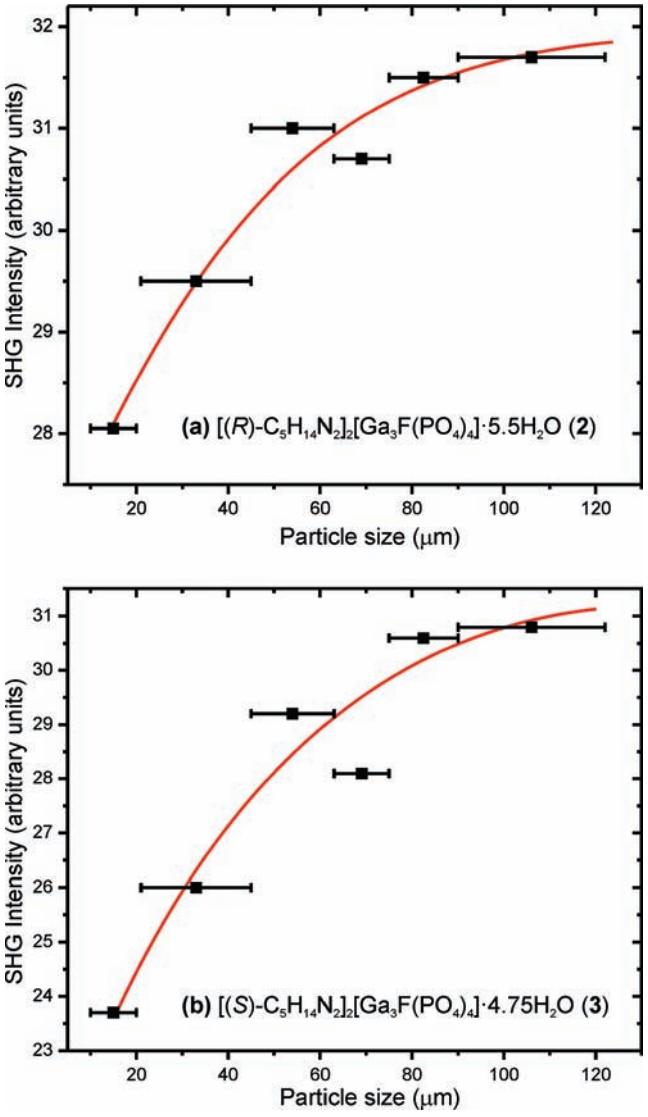

Figure 5. SHG intensity versus particle size data for (a) **2** and (b) **3**. The curves drawn are to guide the eye and are not fits to the data.

disorder owing to its low molecular flexibility and multiple points of interaction between each cation and the inorganic components. Despite this, two disorder mechanisms are observed in the $[2\text{-mpipH}_2]^{2+}$ cations in compound **1**. Inversion symmetry within the cations that reside between $[Ga_3F(PO_4)_4]_n^{4n-}$ layers results in the superimposition of both $[R\text{-}2\text{-mpipH}_2]^{2+}$ and $[S\text{-}2\text{-mpipH}_2]^{2+}$(Figure 6a). The use of a single enantiomer destroys these centers of inversion and crystallographically orders the cations. In addition, the channels in compound **1** are occupied by disordered water molecules and $[2\text{-mpipH}_2]^{2+}$ cations. These cations are highly disordered over six orientations, contain both R-2-mpip and S-2-mpip, and reside on a central inversion center at the origin. The elimination of these inversion centers at 0,0,0 results in the ordering of all $[2\text{-mpipH}_2]^{2+}$ cations in compounds **2** and **3** and forces a reduction in symmetry from *P*-3 to either $P3_1$ or $P3_2$. The outcome of this is the formation of supercells in compounds **2** and **3**, with respect to compound **1**, through a tripling of the *c*-axis (Figure 3).

Counterpoints to the role of template disorder in compound **1** can be found in related systems based upon templated molybdates or sulfated molybdena compounds.

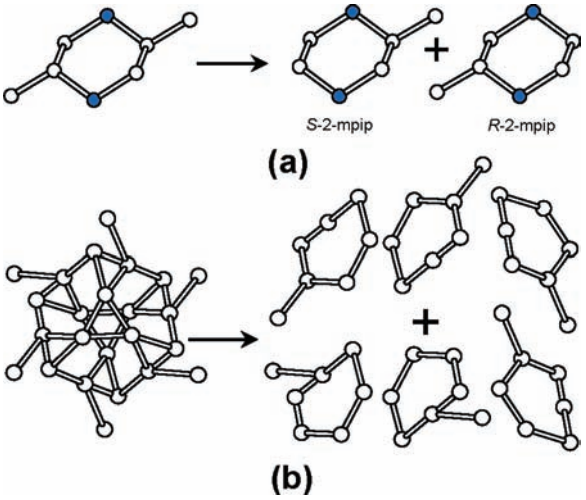

Figure 6. Disorder mechanism for the (a) interlayer and (b) channel $[2\text{-mpipH}_2]^{2+}$ cations in **1**.

$[C_7H_{16}N_2]_2[Mo_8O_{26}]\cdot H_2O$[15] was synthesized using racemic 3-aminoquinuclidine (aqn) under mild hydrothermal conditions contains β-$[Mo_8O_{26}]^{4-}$ anions,[54] and crystallizes in the centrosymmetric space group $P2_1/n$ (No. 14). The asymmetric unit in this structure contains a single-ordered $[S\text{-aqnH}_2]^{2+}$ cation, from which a corresponding $[R\text{-aqnH}_2]^{2+}$ cation is generated through inversion symmetry. Identical syntheses using either enantiomorphically R-aqn or S-aqn result in the noncentrosymmetric compounds $[(R)\text{-}C_7H_{16}N_2]_2[Mo_8O_{26}]$ and $[(S)\text{-}C_7H_{16}N_2]_2[Mo_8O_{26}]$, respectively. The asymmetric units in these structures each contain two unique cations, either two $[R\text{-aqnH}_2]^{2+}$ or $[S\text{-aqnH}_2]^{2+}$ cations. In addition, $[(R)\text{-}C_5H_{14}N_2][(MoO_3)_3(SO_4)]\cdot H_2O$[13] and $[(S)\text{-}C_5H_{14}N_2][(MoO_3)_3(SO_4)]\cdot H_2O$[14] were synthesized using R-2-mpip and S-2-mpip, respectively. Both crystallize in the noncentrosymmetric space group $P2_12_12_1$ (No. 19) and contain a single ordered $[2\text{-mpipH}_2]^{2+}$ cation. However, in contrast to the aqn compounds, the use of racemic 2-mpip does not result in a centrosymmetric analog. Instead, the structure exists as an inversion twin and crystallizes in $P2_12_12_1$.

The three systems presented above display similarities and differences. The use of a racemic source of amines results in highly disordered $[2\text{-mpipH}_2]^{2+}$ cations in compound **1**, ordered $[R\text{-aqnH}_2]^{2+}$ and $[S\text{-aqnH}_2]^{2+}$ cations in $[C_7H_{16}N_2]_2[Mo_8O_{26}]\cdot H_2O$, and the formation of an inversion twin in $[C_5H_{14}N_2][(MoO_3)_3(SO_4)]\cdot H_2O$. However, the use of enantiomorphically pure sources of the respective amines in each system directs crystallization to noncentrosymmetric space groups, crystallographically orders the organic cations, and results in SHG active compounds.

Conclusion

The use of chiral amines is an effective means for the preparation of new noncentrosymmetric organic inorganic hybrid materials. Despite the presence of crystallographic disorder when using a racemic source of the amine, syntheses containing either R-2-mpip or S-2-mpip result in two new noncentrosymmetric compounds with relatively strong SHG activities.

Acknowledgment. The authors acknowledge support from the Research Corporation for Science Advancement.

(54) Lindqvist, I. *Ark. Kemi* **1950**, *2*, 349–355.

A.N.S. gratefully acknowledges support from the National Science Foundation (Award CHE-0215963). J.Y. and P.S.H. thank the Robert A. Welch Foundation (Grant E-1457), ACS PRF 47345-AC10, and NSF (DMR-0652150) for support.

Supporting Information Available: Thermogravimetric traces for compounds **1**−**3**, alternate three-dimensional packing figures for compounds **1**−**3**, and bond valence sums analysis of compounds **1**−**3**. X-ray crystallographic information files (CIF) are available for compounds **1**−**3**. This material is available free of charge via the Internet at http://pubs.acs.org.